Modeling and Simulation of a Microgrid as a Stochastic Hybrid System

Martin Střelec, Karel Macek, Alessandro Abate

***Abstract*—Microgrids (MGs) are small-scale local energy grids. While dedicated to cover local power needs, their structure and operation is usually quite complex. Complexity arises due to a number of factors: in the first instance, a variety of operational modes – among them, MGs can be considered to be operated autonomously whenever the main distribution grid is not available; furthermore, the heterogeneity of energy types in a MG – not exclusively electrical energy, but also thermal for instance; also, the different functions that a MG energy management system has to fulfill – like coordination and dispatching of multiple generation, transfer, transformation and storage devices; finally, the external and internal random factors that affect operations. All these aspects make control and scheduling of a MG quite a challenging task. On the other hand, this widespread complexity leaves much room for improvement on the current state of the art. An advancement on the state of the art requires the development of a realistic model of the system at hand. This work puts forward a model of a MG that is based on the framework of Stochastic Hybrid Systems (SHS). SHS models can capture the interaction between probabilistic elements and discrete and continuous dynamics, and thus promise to be able to tame the complexity of the systems discussed above. This work displays the outcomes of model simulations and discusses potential development of general analysis and synthesis approaches over SHS models (e.g., based on model checking and on approximate dynamic programming) for typical challenges in MGs.**

***Index Terms*—Microgrids, Stochastic Hybrid Systems, Modeling, Simulation**

I. Introduction

Modeling of MGs for control and scheduling purposes has been widely investigated [1], [2], [3] and others. Control problems deal with low-level management of particular devices of a microgrid (e.g., primary voltage control of a turbine) and usually relate to algorithms that operate on the scale of milliseconds. On the other hand, scheduling problems involve the optimal operation at the level of the whole microgrid, which is achieved by coordination and dispatching of various generation, consumption, and storage elements connected to the grid. Scheduling algorithms operate on a minute or hourly scale. Most of the modeling approaches found in the literature are mainly focused on capturing some particular aspects of a given MG, rather than the system as whole: the very concept of MG has been defined in somewhat formal terms in various works [4], each of which has then focused on the description of particular parts and operations of a MG. For instance, a MG concept based on distributed generation and consumption devices has been introduced in [5]. Furthermore, the contributions in [6], [7] have defined a MG via an oriented graph, where edges represented power flows and nodes stood for particular devices.

This paper extends the contribution in [8], where a formal graphical representation of a MG and its relationship with a SHS model has been described in generality. In this paper, we focus on a more formal description of the relationship between the model of a MG and SHS theory. After a discussion on SHS models in Section II, the focus is brought to more practical aspects of MG modeling (Section III) and simulation (Section IV), both of which are demonstrated on a particular example and for specific operational conditions. The paper concludes in Section V with a discussion on potential uses and extensions of the model.

M. Střelec and K. Macek are with the Honeywell Laboratories, Honeywell s.r.o., V Parku 2326/18 , 148 00 Prague,Czech Republic. Email: {martin.strelec,karel.macek}@honeywell.com

K. Macek is also with FNSPE CTU in Prague, Trojanova 13, 120 00 Prague, Czech Republic.

A. Abate is with the Delft Center for Systems and Control, TU Delft - Delft University of Technology, Mekelweg 2, 2628CD Delft, The Netherlands. Email: a.abate@tudelft.nl

II. Stochastic Hybrid Systems

Stochastic Hybrid Systems (SHS) are a class of probabilistic and hybrid dynamical systems. We introduce here a model in continuous-time [9], which is characterized by a hybrid state space defined by two components: discrete modes and continuous states. SHS capture the probabilistic dynamics and the interactions between the two components.

A formal definition of a SHS is introduced in [9], [10], where the model is defined as the collection

$$\mathcal{G} = (\mathcal{Q}, n, A, B, \Gamma, R^{\Gamma}, \Lambda, R^{\Lambda}, \pi),$$

where

- $\mathcal{Q} = \{q_1, q_2, \ldots, q_m\}, m \in \mathbb{N}$ is a countable set of discrete modes representing the discrete state space,
- $n : \mathcal{Q} \to \mathbb{N}$ is a map that determines the dimension of the continuous state space associated with each mode. For $q \in \mathcal{Q}$, the continuous state space is the Euclidean space $\mathbb{R}^{n(q)}$. The hybrid state space is then $\mathcal{H} = \cup_{q\in\mathcal{Q}}\{q\} \times \mathbb{R}^{n(q)}$,
- $A = \{a(q,\cdot) : \mathbb{R}^{n(q)} \to \mathbb{R}^{n(q)}, q \in \mathcal{Q}\}$ is the collection of drift terms of the SDEs governing the continuous dynamics,
- $B = \{b(q,\cdot) : \mathbb{R}^{n(q)} \to \mathbb{R}^{n(q)}, q \in \mathcal{Q}\}$ is the collection of diffusion terms of the SDEs governing the continuous dynamics,
- Γ is a subset of the hybrid state space $\mathcal{H}$ defined as $\Gamma = \cup_{q\in\mathcal{Q}}\{\Gamma_q\}_q$, where $\Gamma_q = \cup_{q'\neq q\in\mathcal{Q}}\gamma_{qq'}$ is a closed set composed of $m-1$ disjoint guard sets $\gamma_{qq'}$, which cause forced transitions from mode q to mode $q' \neq q$,
- $R^{\Gamma} : \mathcal{B}(\mathbb{R}^{n(\cdot)}) \times \mathcal{Q} \times \mathcal{H} \to [0,1]$ is the reset stochastic kernel associated with Γ. Specifically, $R^{\Gamma}(\cdot|q',(q,x))$

is a probability measure defined on $\mathbb{R}^{n(q')}\backslash\Gamma_{q'}$, which describes the probabilistic reset of the continuous state when a jump from mode q to q' occurs from $x \in \gamma_{qq'}$,
- $\Lambda : \mathcal{H}\backslash\Gamma \times \mathcal{Q} \to \mathbb{R}^+$ is the transition intensity function governing spontaneous transitions. Specifically, for any $q \neq q' \in \mathcal{Q}, \lambda_{qq'}(x) := \Lambda((q,x),q')$ is the jump rate from mode q to mode q' when $x \in \mathbb{R}^{n(q)}\backslash\Gamma_q$,
- $R^\Lambda : \mathcal{B}(\mathbb{R}^{n(\cdot)}) \times \mathcal{Q} \times \mathcal{H}\backslash\Gamma \to [0,1]$ is the reset stochastic kernel associated with Λ. In particular, $R^\Lambda(\cdot|q',(q,x))$ is a probability measure defined on $\mathbb{R}^{n(q')}\backslash\Gamma_{q'}$ that describes the probabilistic reset of the continuous state when a jump from mode q to q' occurs from $x \in \mathbb{R}^{n(q)}\backslash\Gamma_q$,
- $\pi : \mathcal{B}(\mathcal{H}) \to [0,1]$ is a probability measure concentrated on $\mathcal{H}\backslash\Gamma$ that describes the initial state distribution.

Trajectories are initialized randomly according to a probability distribution π. Within any given mode $q \in \mathcal{Q}$, the evolution of the continuous variables is characterized as the solution of a stochastic differential equation of the form

$$dx(t) = a(q(t),x(t))dt + b(q(t),x(t))dw(t) \ ,$$

where $w(t)$ is a standard, $n(q)$-dimensional Wiener process (considering a driving Wiener process with a different dimension is also possible). Mode changes are due to events related to trajectories entering the deterministic spatial guard set Γ, or alternatively to random arrivals due to Poisson processes with a spatially-dependent rate Λ. Upon changing the discrete mode, trajectories are reset probabilistically according to the measures R^Γ and R^Λ, respectively.

Further details about the syntax, semantics, and properties of a SHS can be found in [9], [10]. In particular, we refer to the cited literature for the measure-theoretical properties of the model, and for the elucidation of related concepts such as the σ-algebra $\mathcal{B}$ over a probability space. With a more practical objective, specific terms of the model will be discussed more in depth, within the context of a MG, in Sections III and IV.

III. Modeling of a Microgrid as a Stochastic Hybrid System

A. The system under study

Figure 1 displays the configuration of the considered MG. The MG is connected to the main distribution grid, which feeds the local power network with electricity. In this work we assume that the main distribution grid is operated by a transmission and system operator (TSO) – more generally, depending on many factors such as electricity market structure, geographical location, etc., other subjects or participants to the electricity market (e.g., an electric utility company) can perform as the main grid operator. Two local generation sources are additionally considered: a microturbine and a wind turbine. A microturbine is controllable device that consumes natural gas from a gas pipeline (gas utility) and that produces not only electrical but thermal energy (heat) as well. Thermal energy is thereafter transported to the heating system. In this article, for the sake of simplicity only the electrical component of the microturbine will be considered. A wind turbine represents an uncontrollable generation device with a stochastic behavior. Furthermore an electrical energy storage

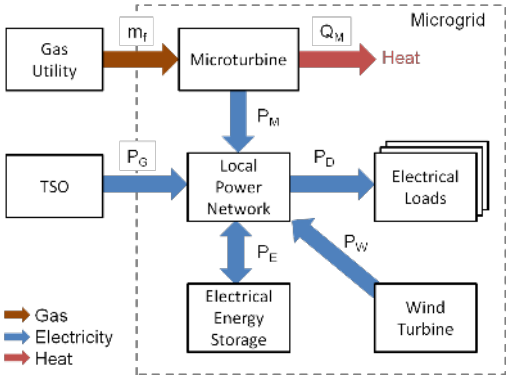

Fig. 1. Example of a microgrid, taken as a case study for this work.

serves for the startup of the microturbine whenever in island mode[1], as well as for power balancing during energy peak periods. Furthermore, several electrical loads are connected to the local power network. These loads are stochastic in nature and cannot be rescheduled or curtailed.

B. Discrete components and dynamics

Single MG elements have characteristic discrete modes that affect not only their own continuous behavior, but also the behavior of whole MG. The following list summarizes the discrete modes of the single devices:

- Local Power Network *(L)* = {*On: 1*, *Off: 0*}
- Distribution Grid *(G)* = {*Connected: 1*, *Disconnected: 0*}
- Microturbine *(M)* = {*Off: 0*, *Start: 1*, *On: 2*, *Shut down: -1*}
- Wind Turbine *(W)* = {*Connected: 1*, *Disconnected: 0*}
- Electrical Energy Storage *(E)* = {*Supply: 1*, *Store: 0*, *Load: -1*}
- Electrical Loads *(D)* = {*Connected: 1*, *Disconnected: 0*}

The set $\mathcal{Q}$ of discrete modes of the whole MG is given as a subset of the cross product of the discrete models of the devices $L \times G \times M \times W \times E \times D$. Figure 2 shows explicitly an automaton-like structure, characterizing the discrete dynamics of the considered system. The nodes of the graph represent the discrete modes $q \in \mathcal{Q}$, whereas the edges represent transitions among the discrete modes. Each node is labeled by unique number, which denotes the corresponding discrete mode in the model.

The edges of the graph denote possible discrete jumps and can be of two kinds: either due to guard conditions in Γ, or due to spontaneous jumps in Λ. More specifically, guard conditions $\gamma_{q,(\cdot)}$ constitute forced transitions from mode q to other discrete modes, which occur when the continuous dynamics enter the set $\gamma_{q,(\cdot)}$. For example, the system jumps from mode [1,1,1,1,0,1] (microturbine in *Start* mode) to the mode [1,1,2,1,0,1] (microturbine in *On* mode) when the angular speed of the turbine ω is greater than or equal to its nominal speed ω_{nom}, namely $\gamma_{4,7} : \omega \geq \omega_{nom}$. On the other

[1]A local electric network is said to be in island mode when it is not connected to the main distribution grid (e.g. because of a blackout) nor to other local grids, but it is still able to operate autonomously.

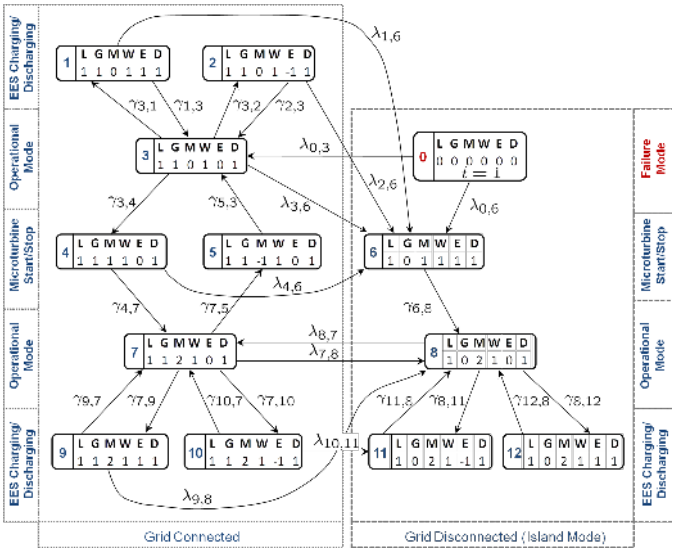

Fig. 2. Automaton-like representation of the discrete components of the MG. The left column refers to the grid in the connected mode (G=1), whereas the right one to the disconnected one (island model, G=0). Rows in the figure refer to operational modes of specific devices (namely, E and M). The rates and guards appearing by the edges are discussed in the text.

hand spontaneous jumps $\lambda_{q,(\cdot)} \in \Lambda$ represent probabilistic events that may occur anywhere within the continuous state space $\mathbb{R}^{n(q)}$ of a given discrete mode $q \in \mathcal{Q}$. The probability associated to a spontaneous jump from the current discrete mode q to another one is given by a non-homogeneous exponential distribution, characterized by the intensity function $\lambda_{q,(\cdot)}$, which can depend on the continuous state in $\mathbb{R}^{n(\cdot)}$ and on time t. Examples of intensity functions are given in Section IV.

There are further spontaneous transitions to the *Off* mode of the LPN ($L = 0$), depicted as the top mode on the right of Figure 2 (the incoming rates $\lambda_{(\cdot),0}$ are not explicitly shown – an example will be given in Section IV). Namely, the system can jump to a failure mode from any other mode due to the following two causes:

- an *abrupt failure* has happened, for some reason (often exogenous to the system). This case represents a spontaneous transition that is defined by a probabilistic function.
- a *large power unbalance* has occurred in the power network of the local MG, which leads to the activation of power protections and to the disconnection of the local power network. This event can be characterized by a conditional probability function, where the probability to jump grows as the power unbalance rises.

In both cases, within mode $L = 0$ an internal clock associated to the failure state is reset to zero, $t = 0$. The clock dynamics is defined by the simple differential equation $\dot{t} = 1$ and, together with the transition rates $\lambda_{0,3}$ and $\lambda_{0,6}$, characterizes the dwelling time within the failure mode.

When the system jumps to a new discrete mode $q \in \mathcal{Q}$, the continuous state can be reset probabilistically over the target mode, that is over $\mathbb{R}^{n(q)}$. Probabilistic kernels are used for the reset of the continuous state, namely R^{Γ} is used after forced transitions, whereas R^{Λ} is used after spontaneous jumps. While in general state resets can be useful in situations such as when the grid goes from a *Connected* to a *Disconnected* mode and some of the electrical loads get off line, in this work for the sake of simplicity we assume that both reset maps are deterministic and equal to the identity map, which indicates that the continuous state does not change value upon mode switches.

C. Continuous components and dynamics

Each discrete mode $q \in \mathcal{Q}$ is endowed with specific continuous dynamics, which are characterized by the physical properties of the specific elements in the given mode.

1) Power balance equation: This equation determines the relationship between power generation and the power on the demand side. The power unbalance ΔP can be written as the following algebraic equation

$$\Delta P = P_G + P_M + P_W + P_E - P_D, \tag{1}$$

and expressed in the differential form as follows

$$\Delta \dot{P} = \dot{P}_G + \dot{P}_M + \dot{P}_W + \dot{P}_E - \dot{P}_D, \tag{2}$$

where P_G represents the grid power, P_M is the microturbine power, P_W characterizes the wind turbine power, P_E is the power transfered to/from the electrical storage, and P_D is the power demanded by the loads. Equation (2) inherits specific terms that depend on the current discrete mode, as per Figure 2. Within each discrete mode, the drift term A and the diffusion term B are determined based on the continuous dynamics and on the uncertainty for particular terms of Equation (2). In the following, specific terms of Equation (2) are described in more detail.

2) Grid Power: Whenever the MG is connected to the main distribution grid, the grid power P_G compensates the power unbalance ΔP by a feedback mechanism, which can be defined as follows:

$$\dot{P}_G = k_G \cdot \Delta P, \tag{3}$$

where k_G is a proportional coefficient. The feedback in Equation (3) is mainly implemented via primary frequency control [11]. If the MG is operating in island mode, then the power P_G is constantly equal to zero.

3) Microturbine: A microturbine element is considered as small gas turbine, the behavior of which can be characterized by a number of discrete modes [12] and by related continuous dynamics. As mentioned above, a gas turbine distinguishes the following four modes:

- *Off* - the turbine is in the off mode.
- *Start* - the turbine is starting up. The power generator is used for the rotation of the turbine. Whenever the turbine reaches a predefined RPM level, it starts the fuel ignition. Then the turbine is first warming up, and afterwards is synchronized with the distribution grid. In this stage the turbine is consuming electricity and some fuel, however it is not producing power yet.
- *On* - the turbine is connected to the grid, consumes natural gas, and generates power.

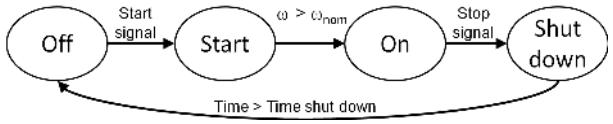

Fig. 3. Switching sequence for the discrete modes of the microturbine.

- *Shut down* - the ignition process has been stopped, the generator is spinning over the turbine at constant RPM, and the turbine is cooling down. After a predefined time, the generator is switched off and the turbine is smoothly decelerated.

The microturbine changes its discrete modes according to the scheme in Figure 3. The microturbine model jumps from the *Off* to the *Start* mode when a Start signal is active. The model remains in the *Start* mode until the rotational speed ω of the turbine is lower than nominal speed ω_{nom} (condition $\gamma_{4,7}$ is valid). Afterwards, the microturbine commutes into the *On* mode, where it stays until a Stop signal becomes active. Thereafter the system jumps to the *Shut down* mode, where it spends a predefined time, after which it switches back to the *Off* mode.

In the literature it is common to refer to two kinds of gas turbine models, based respectively on a model by Rowen [13] and on one by the IEEE [14]. Both dynamical models incorporate mechanical, combustion, and electrical dynamics, and are too complex for our demonstrative purposes. We thus adopt simpler, non-linear dependencies, where the turbine mechanics represents its only dynamics, which can be captured by the following first order differential equation:

$$J \cdot \frac{d\omega}{dt} = (T_M - T_E - F_V), \tag{4}$$

where J is the moment of inertia, ω denotes the angular velocity, T_E refers to the electrical torque, T_M is the mechanical torque, F_V is the force due to viscous friction and finally ω represents the angular speed. The above mechanical part (4) is the same for all the four discrete modes considered for the microturbine. For all the discrete modes, the viscous friction is $F_V = -k_v \cdot \omega$, where k_v is the viscous coefficient.

In the *Start* mode, a power generator is used as an electric motor and is increasing the turbine velocity to a predefined RPM. In this configuration the mechanical torque is taken to be equal to zero – $T_M = 0$ – because the minimal fuel flow maintains the combustion process but does not produce a mechanical torque. Thus the electrical torque represents the driving force for the rotation of the turbine, and is defined as

$$T_E = a_0 + a_1 \cdot P_M + a_2 \cdot P_M^2, \tag{5}$$

where a_0, a_1, a_2 are real constants. Since the generator in this mode is connected to the electric motor, P_M represents the consumed power. When the turbine is rotating at a predefined and nominal RPM ω_{nom}, it starts to ignite fuel, warms up, and is synchronizing its voltage phase and frequency with the local power grid, however it still does not supply the microgrid with power. Afterwards the turbine is switched to the operational *On* mode, where the generator produces power and the microturbine is driven by a combustion process. The mechanical torque represents the driving force for the rotation of the turbine, and can be characterized with the following polynomial:

$$T_M = a_3 + a_4 \cdot m_f + a_5 \cdot m_f^2 - a_6 \cdot \omega, \tag{6}$$

where a_3, a_4, a_5, a_6 are real constants, m_f is the fuel flow and ω is the angular velocity. The electrical torque acts along the mechanical one, and is decelerating the turbine angular velocity. The electrical torque can be defined by a second-order polynomial

$$T_E = a_7 + a_8 \cdot \omega + a_9 \cdot \omega^2, \tag{7}$$

where a_7, a_8, a_9 are real constants and ω is the current angular velocity. The generated power depends on the angular velocity and can be expressed as

$$P_M = a_{10} + a_{11} \cdot \omega + a_{12} \cdot \omega^2, \tag{8}$$

where a_{10}, a_{11}, a_{12} are real constants. For the sake of simplicity, no power electronics (e.g. rectifier, inverter etc.) have been considered – a more complex model of the generator can be found in [15]. Besides electricity, the gas turbine produces energy from heat, which is subsequently transfered to a hot water circuit. The amount of produced heat energy is defined by the function

$$Q_M = a_{13} + a_{14} \cdot m_f + a_{15} \cdot m_f^2, \tag{9}$$

where m_f is the fuel flow, and a_{13}, a_{14}, and a_{15} are real constants.

The *Shut down* mode has a behavior that is analogous to the *Start* mode: the fuel combustion is stopped, the generator is spinning the turbine on a predefined RPM, and the turbine is smoothly cooling down. After a given time, the generator is switched off and the turbine speed is naturally decelerated to zero.

4) Wind Turbine: We adopt a standard nonlinear static model that is widely adopted in the literature [11]:

$$P_W = \frac{1}{2} \cdot \rho \cdot R^2 \cdot u^3 \cdot C_p(\eta, \theta), \tag{10}$$

where ρ denotes the air density, R is the blade radius, u denotes the wind speed, and C_p is an efficiency function depending on θ (the wind direction) and on the parameter $\eta = \frac{\omega R}{u}$, where ω is the speed of the blade tip. A differential relation can be obtained from (10), cfr. Appendix A. A hybrid automaton model for the wind turbine has been introduced in [16], and has been characterized by a number of discrete modes. For the sake of simplicity, we consider only two discrete modes: *Connected* and *Disconnected*. In the *Connected* mode, we consider the wind turbine to be connected to the local power network and to be operating in the power optimization area[2]. When on the other hand the wind turbine is *disconnected* from the local power network, then it does not feed the microgrid with power.

[2]The turbine is in the power optimization area when the speed of its blade tip that is less than a maximal tip speed.

5) Electrical Energy Storage: This device can store electrical energy over time. We consider a simplified storage model inspired by [1], which expresses the stored energy P_{ES} as

$$\frac{dP_{ES}}{dt} = -\eta \cdot P_E - P_{LOSS}, \tag{11}$$

where η denotes power exchange efficiency, P_E is the power exchanged between the storage device and the local power network, and P_{LOSS} denotes power losses associated to the storage. Notice that the variable P_{ES} is the state variable determining the energy level stored in the storage device, whereas the variable P_E denotes an input variable quantifying the power supplied (loaded) from (over) the storage device in connection with the local power network.

The power exchange efficiency parameter is defined as

$$\eta = \begin{cases} \eta_s, & \text{for the } \textit{Supply} \text{ mode } (P_E > 0), \\ 0, & \text{for the } \textit{Store} \text{ mode } (P_E = 0), \\ \eta_l, & \text{for the } \textit{Load} \text{ mode } (P_E < 0). \end{cases} \tag{12}$$

6) Electrical Loads: Electrical loads are characterized by dynamics that are stochastic in nature and can be modeled by stochastic differential equations. The Uhlenbeck-Ornstein model is a suitable candidate [17] for the modeling of the continuous dynamics of electrical loads in the *Connected* mode:

$$dP_D = \alpha \cdot (m - P_D) \cdot dt + \sigma_D \cdot dW, \tag{13}$$

where m is a given load profile, α represents a tracking coefficient, σ_D is a variation coefficient, and dW denotes the Wiener process. In the case of the *Disconnected* mode, the dynamics of electrical loads is trivial as

$$P_D = 0, \quad dP_D/dt = 0. \tag{14}$$

D. Uncertainty

There are two entities in the model that are affected by stochasticity in the considered case study: the dynamics of the electrical loads and the wind turbine power. The electrical loads are modeled as systems with no input, and the stochasticity acts endogenously over the power dynamics, as per (13). On the other hand, the wind turbine is considered as a deterministic system as in (10), but it is affected by stochastic inputs. These input depend on the wind direction θ and the wind speed u. There are several modeling approaches in the literature encompassing these two inputs. Modeling of wind variability via discrete Markov chains is described in [18], whereas [19] has introduced a weather prediction model based on Bayesian networks. Alternative approaches are based on time series models [20]. When considering optimal placement of the wind turbine, then generated power depends on the wind speed u only. In this latter case, wind speed u can be modeled as simple one-dimensional stochastic differential equation [21], such as

$$du(t) = -\frac{u(t) - \bar{u}(t)}{T} \cdot dt + \kappa \cdot \bar{u}(t) \cdot \sqrt{2/T} \cdot dW(t) \ , \tag{15}$$

where $\bar{u}$ denotes hourly averages of wind speed, κ is factor depending on the geographical location of the wind turbine, and the parameter $T = L/\bar{u}$, where L is the turbulence length scale [21].

E. Model initialization

The presence of uncertainty leads to limited information about the initial condition of the model. The initialization of a trajectory of the model over the hybrid state space (this involves both the initial discrete mode and the initial value of the continuous state) is given by a probabilistic measure π (i.e., a uniform probability distribution over a subset of $\mathcal{H}$). Different initial conditions of the model can lead to different trajectories of the system $\mathcal{G}$ over the hybrid state space $\mathcal{H}$.

IV. Simulation of a Microgrid by a Stochastic Hybrid System

This section begins with a description of a possible operation of the system and continues with an illustration of the model from the perspective of stochastic hybrid systems theory. Thereafter, a simulation of the microgrid in the considered operation is shown and discussed.

A. System operation

Let us outline a possible condition occurring in the MG. The MG starts in the operation mode ($L = 1, G = 1$) and is connected to the main distribution grid. The wind turbine and electrical devices are initially connected to the local power network. Suddenly a blackout of the main distribution grid occurs and the MG is consequently disconnected from the main distribution grid ($G = 0$), and the electrical loads are been supplied by the wind turbine and by the electrical energy storage device. Within this situation, the microturbine starts to operate again, and is switched to its *On* mode after it reaches its nominal RPM. When the microturbine is in operational mode, it feeds the electrical loads and the electrical energy storage device is disconnected. From this situation, assume that the electrical loads excess the maximal performance of the microturbine (a power unbalance occurs): the power difference between consumption and generation side has augmented and the local power network is shut down ($L = 0$).

B. Formulation of the system operation by a SHS model

The considered operation of the MG is now explained in terms of a stochastic hybrid system model.

At the outset of the case study the MG is connected to the grid. The wind turbine and the electrical loads are connected to the local power network. Therefore the system is in the discrete mode[3] [1,1,0,1,0,1], which is represented by node 3 in Figure 2. Associated to this mode is a continuous domain, defined by the variable $X = (\Delta P, P_G, P_M, \omega, P_W, C_P, P_{ES}, P_D, u)$. According to the equations described in Section (III-C), it is possible to explicitly write out the drift terms A and the diffusion terms B for the continuous dynamics, as reported in Table I. These terms fully characterize the evolution of the system state over the continuous state space. In this table, the number $i, i = 1, \ldots, 9$ indexes a particular position of the continuous vector variable for the given discrete mode 3.

[3]Recall that a mode is characterized by the discrete value of the vector [Local Power Network, Distribution Grid, Microturbine, Wind Turbine, Electrical Energy Storage, Electrical Loads].

TABLE I
DRIFT (A) AND DIFFUSION (B) TERMS FOR THE CONTINUOUS DYNAMICS WITHIN DISCRETE MODE $[1,1,0,1,0,1]$ (MODE 3).

A(3,X)	B(3,X)
$a_1(3,X) = \dot{P}_G + \dot{P}_W - \dot{P}_D$	$b_1(3,X) = 0$
$a_2(3,X) = k_G \cdot \Delta P$	$b_2(3,X) = 0$
$a_3(3,X) = 0$	$b_3(3,X) = 0$
$a_4(3,X) = -F_V$	$b_4(3,X) = 0$
$a_5(3,X) = \frac{3}{2}\cdot\rho\cdot R^2\cdot u^2\cdot\frac{du}{dt}\cdot C_p(\eta,\theta)$ $+\frac{1}{2}\cdot\rho\cdot R^2\cdot u^3\cdot\frac{dC_p(\eta,\theta)}{dt}$	$b_5(3,X) = 0$
$a_6(3,X) = \frac{dC_p}{d\eta}\cdot\frac{d\eta}{dt} + \frac{dC_p}{d\theta}\cdot\frac{d\theta}{dt}$	$b_6(3,X) = 0$
$a_7(3,X) = -P_{LOSS}$	$b_7(3,X) = 0$
$a_8(3,X) = \alpha\cdot(m - P_D)$	$b_8(3,X) = \sigma_D\frac{dW}{dt}$
$a_9(3,X) = -\frac{u-\hat{u}}{T}$	$b_9(3,X) = \kappa\bar{u}\sqrt{\frac{2}{T}}\frac{dW}{dt}$

After some time, a blackout occurs in the main distribution grid. This leads to the MG operating in island mode (namely, disconnected from main distribution grid). The loads are supplied energy by the wind turbine and by the electrical energy storage, whereas the microturbine is in the *Start* mode and is accelerating towards the nominal angular velocity ω_{nom}. Dynamically, the model has jumped from the discrete state $[1,1,0,1,0,1]$ to $[1,0,1,1,1,1]$ (mode 6 in Figure 2), in a spontaneous manner. Such a spontaneous occurrence can be modeled by a Poisson arrival with constant rate $\lambda_{3,6}$ as in Figure 2. This simple arrival process can be generalized in many ways: for instance, $\lambda_{3,6}$ can be assumed to be a function of weather, external conditions, or other relevant factors; alternatively, the transition rate can be a function of the frequency of the main grid, where the frequency is modeled as a stochastic process.

Within the new discrete mode $[1,0,1,1,1,1]$, the continuous domain is the same (and has the same dimension) as in the previous mode (in general, by definition it could be different). However, the associated drift and diffusion terms have to be updated – they are not described here for the sake of space: for more details, we refer the reader to the Appendix A, where the continuous dynamics for the various discrete modes are schematically captured within a graphical structure.

Recall that the microturbine is accelerating: when it reaches the nominal angular velocity ω_{nom}, it is switched to the *On* mode and the model commutes from the discrete mode $[1,0,1,1,1,1]$ to mode $[1,0,2,1,0,1]$ (mode 8 in Figure 2). This jump is forced and is captured by the guard $\gamma_{6,8}$, which is written out explicitly as the following condition: $\omega \geq \omega_{nom}$. (Incidentally, notice that $\gamma_{6,8} = \gamma_{4,7}$, as introduced in Section III-B.) Within the new mode, the microturbine takes over the balance of the power difference ΔP in the MG, while the wind turbine supports the MG with a power generation that is stochastic in nature. The electrical loads are now connected to the MG, while on the other hand the main distribution grid and the energy storage are disconnected.

Let us now consider a spontaneous jump from this discrete mode to the failure mode $[0,0,0,0,0,0]$, namely mode 0 in Figure 2, characterized by $L = 0$, which is caused by a *large power unbalance* – this occurrence was mentioned in subsection III-B. The probability associated to this event can

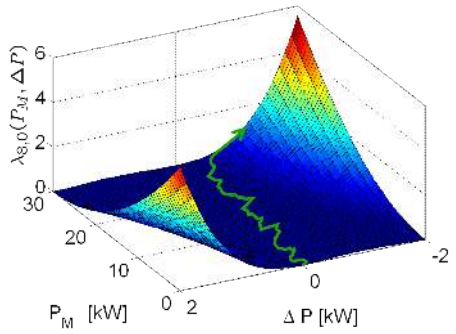

Fig. 4. Transition rate $\lambda_{8,0}(P_M, \Delta P)$ and sample path (green line).

be modeled as a function of the actual power difference ΔP and of the actual power generated by the microturbine P_M. The transition rate function $\lambda_{8,0}(\Delta P, P_M)$ is explicitly defined as the following positive quantity:

$$\lambda_{8,0}(\Delta P, P_M) = \left[\Delta P \cos\left(\frac{\pi}{24}\right) - \left(P_M - \frac{P_{M,max}}{2}\right)\sin\left(\frac{\pi}{24}\right)\right]^2 \left(\frac{\Delta P}{3}\right)^2, \quad (16)$$

where $P_{M,max}$ is the maximal possible power that can be generated by the microturbine. Figure 4 shows graphical representation of the transition rate function $\lambda_{8,0}(\Delta P, P_M)$. Whenever the load is smaller than the power generated, the term ΔP is positive. If in this situation the microturbine is generating a power level that is close to zero, it is not able to compensate the positive ΔP via generation reduction, consequently the jump likelihood into the failure mode is rising. An analogous situation occurs if the power difference ΔP is negative and the turbine operates close to the maximal performance. Figure 4 displays a sample path, marked by a green line, overlaid on the rate function. The microturbine is increasing the generation according to the rising load. When the microturbine reaches its maximal generation limit, the power difference ΔP is increasing and the probability of the jump into the failure mode is rising, until this event occurs.

C. Simulation of the SHS model of the microgrid

There exist a number of simulation tools for deterministic hybrid systems. However, only some of them can feature stochastic components. For example, Ptolemy II [22] is able to capture probabilistic continuous and discrete dynamics – the only limitation is that the transitions are only based on guards and the consequent reset is exclusively deterministic. Therefore this tool can be useful only for the simulation of a subclass of SHS. Similar comments hold for other simulation tools, like CheckMate [23], and the Ellipsoidal Toolbox [24]: they often allow for uncertain (rather than probabilistic) components. There is the need for a tool aimed at general SHS simulations.

In this work we have employed a Simulink environment for the simulation of the developed MG model. The Simulink model of the MG was created based on the equations described in Section III-C. We have simulated the behavior described

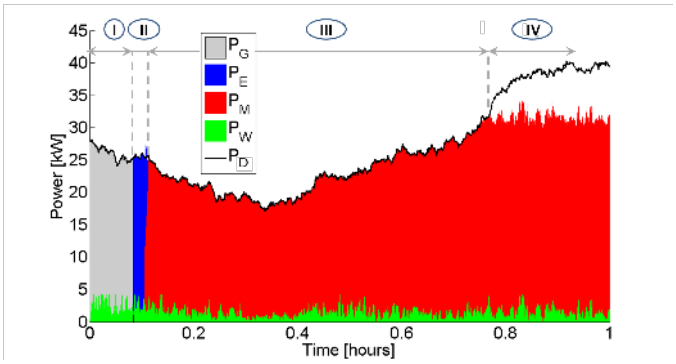

Fig. 5. Power composition in the MG for the situation under study.

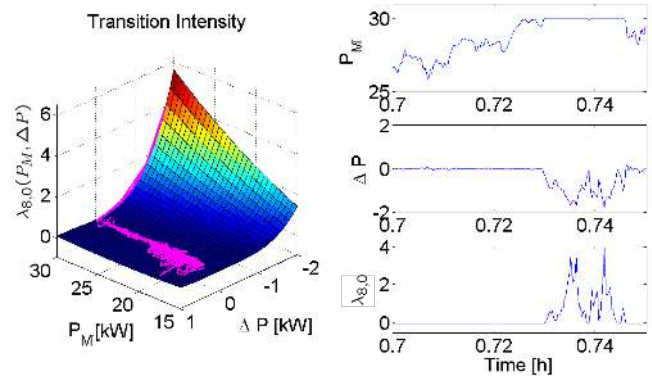

Fig. 6. Transition Rate Function $\lambda_{8,0}(P_M, \Delta P)$ and sample outputs.

in (the previous) Section IV-A. Figure 5 displays the power composition in the MG (loaded and generated power) over one hour of simulation. The grid power P_G is marked with gray color, whereas the blue color denotes the power from electrical energy storage P_E, and red is for the power generated by the microturbine P_M, green color marks the power from the wind turbine P_W, and finally and the black line is the electrical load P_D. The simulation output for the power is divided into four intervals, which are marked with roman numerals in Figure 5. These intervals represent the results of the simulation for the specific discrete modes described in the previous section. In the intervals $I - III$, the MG is in operational mode and can fully supply the connected electrical loads. In the interval IV, the electrical loads have a higher capacity than that of the generators, and the probability of entering the failure mode is rising.

Figure 6 displays the shape of the transition intensity function $\lambda_{8,0}$ and sample outputs of selected continuous variables (inclusive of the value of $\lambda_{8,0}$) in time. These samples of the continuous variables are taken from time interval where the microturbine performance reaches its maximum and the electrical load P_D (and the power difference ΔP) is still rising. Before this time interval, the electrical load is covered by the local generation devices or by the main distribution grid and the value of the transition rate function $\lambda_{8,0}$ is close to zero. After this time interval, the system is likely to jump to the failure state with a probability that depends on transition rate function $\lambda_{8,0}$. On the left-hand side of the figure, the values of the function $\lambda_{8,0}$ are displayed over one sample path of the electrical load (a sample path is one realization of the load profile in Equation (13)), which is marked with a magenta line. On the right-hand side, the evolution of the transition rate function $\lambda_{8,0}$, as well as the trends of the independent variables ΔP and P_M, are displayed. According to (16), the intensity function $\lambda_{8,0}$ rises when the power difference ΔP is becoming more negative and the microturbine power P_M is close to its maximal performance. In this situation the probability of a spontaneous jump into failure mode increases as well.

Due to space limitations we do not display here the dynamics of other variables of the model in their different operation modes. Based on the underlying initial probability distribution and stochastic components, it is possible to obtain traces of executions by resorting to known Monte-Carlo techniques.

V. Potential Studies and Applications

There are many practical problem formulations that can be considered in a MG. A suitable choice of the modeling framework can play a significant role in tackling such problems: we argue that SHS models can contribute to such a framework.

Generation scheduling constitutes a typical problem to be solved within a MG. An important goal of a MG energy management system is to minimize the operational costs, under satisfaction of supplies to all the loads. This can be achieved by suitable scheduling and utilization of internal and external energy sources. The adoption of a SHS framework for the modeling of MGs can allow leveraging methods from SHS theory, e.g. stochastic optimal control and dynamic programming, for scheduling problems. To attain scheduling optimality we also envision using randomized approaches like the scenario approach [25]. These techniques can help optimizing over random quantities such as wind speed (15) or power loads (13). Furthermore, model checking methods, for instance invariance analysis, can assess the probability that the system under study satisfies the supply to all the loads.

A MG can participate in *demand response* programs and this can offer the opportunity to look into partial load reduction to the TSO for contracted award. For the TSO, demand response (in particular real-time demand response) represents an alternative to the traditional ancillary services for distributed grid stabilization. A MG reaction to a demand response event can be computed based on methods like dynamical programming, randomized techniques, etc. Model checking methods like reachability analysis can further quantify the probability that the system under study reaches any undesired state, such as poor operation schedule or inappropriate reaction to a demand response events, which can lead to large power unbalance in a MG, and as a consequence to the collapse of the local power network and to the system entering a failure mode.

VI. Conclusions

This work has presented a novel approach to modeling MGs, with SHS as promising modeling framework. An SHS model instance of a MG has been introduced and simulations of an operational condition for the MG has displayed that the model

exhibits a reasonable behavior. This suggests that the model can be used as a framework for more advanced analysis and control synthesis problems.

Further research is intended to be developed towards adding other elements to the model and to design an optimized control and scheduling mechanism for MG energy optimization.

ACKNOWLEDGMENTS

This research has been supported by the European Commission under the project MoVeS, FP7-ICT-257005. A. Abate further acknowledges the support of the European Commission via Marie Curie grant MANTRAS 249295, and via NoE HYCON2 FP7-ICT-2009-5 257462.

REFERENCES

[1] A. Parisio and L. Glielmo, "Energy efficient microgrid management using model predictive control," in *50th IEEE Conference on Decision and Control and European Control Conference (CDC-ECC 2011)*, 2011, pp. 5449–5454.

[2] R. Minciardi and R. Sacile, "Optimal control in a cooperative network of smart power grids," *IEEE Systems Journal*, vol. 6, no. 1, pp. 126–133, 2011.

[3] M. Faisal, "Microgrid modelling and online management," Ph.D. dissertation, Helsinki University of Technology, 2008.

[4] S. Chowdhury, S. Chowdhury, and P. Crossley, *Microgrids and Active Distribution Networks*, ser. Renewable Energy Series. The Institution of Engineering and Technology, 2009, vol. 6.

[5] R. Lasseter and P. Paigi, "Microgrid: a conceptual solution," in *35th Annual Power Electronics Specialists Conference (PESC 2004)*, vol. 6, June 2004, pp. 4285–4290.

[6] S. Bolognani and S. Zampieri, "Distributed control for optimal reactive power compensation in smart microgrids," in *50th IEEE Conference on Decision and Control and European Control Conference (CDC-ECC 2011)*, Orlando (FL), USA, December 2011, pp. 6630–6635.

[7] H. Liang, B. Choi., A. Abdrabou, W. Zhuang, and X. Shen, "Decentralized economic dispatch in microgrids via heterogeneous wireless networks," *IEEE Journal on Selected Areas in Communications*, 2011.

[8] K. Macek and M. Strelec, "Micro-grid as a stochastic hybrid system - two formal frameworks for advanced computing," in *Proceedings of SMARTGREENS*, 2012, pp. 141–144.

[9] M. Bujorianu and J. Lygeros, "Toward a general theory of stochastic hybrid systems," *Lecture Notes in Control and Information Sciences (LNCIS)*, vol. 337, pp. 3–30, 2006.

[10] A. Abate, J.-P. Katoen, M. Fraenzle, and M. Prandini, "D1.1 report on modeling frameworks, model composition and bisimulation notions," MOVES Consortium, Tech. Rep., 2011. [Online]. Available: http://www.movesproject.eu/deliverables/WP1/D1.1.pdf

[11] J. Machowski, J. Bialek, and J. Bumby, *Power System Dynamics - Stability and Control*. John Wiley & Sons, Ltd, 2008.

[12] M. Tigges, "Modellbasierte analyse zur verbesserung der elektrischen energiebereitstellung zuknftiger offshore-windparks mittels biogastechnologie," Ph.D. dissertation, Universitaet Paderborn, 2010.

[13] I. Rowen, "Simplified mathematical representations of heavy-duty gas turbines," *Journal Of Engineering For Power*, vol. 105, no. 4, pp. 865–869, 1983.

[14] S. Yee, J. Milanovic, and F. Hughes, "Overview and comparative analysis of gas turbine models for system stability studies," *IEEE Transactions on Power Systems*, vol. Vol. 23, pp. 108 – 118, 2008.

[15] D. Gaonkar and R. Patel, "Modeling and simulation of microturbine based distributed generation system," in *2006 IEEE Power India Conference*, 2006, p. 5.

[16] J. Tzanos, K. Margellos, and J. Lygeros, "Optimal wind turbine placement via randomized optimization techniques," in *Power Systems Computation Conference (PSCC 2011)*, Stockholm, Sweden, 2011.

[17] R. Weron, B. Kozlowska, and J. Nowicka-Zagrajek, "Modeling electricity loads in California: a continuous-time approach," *Physica A*, vol. 299, p. 344, 2001.

[18] J. Mur-Amada and A. Bayod-Rujula, "Wind power variability model – part ii – probabilistic power flow," in *9th International Conference on Electrical Power Quality and Utilisation (EPQU 2007)*, Oct 2007, pp. 1–6.

[19] A. Cofo, R. Cano, C. Sordo, and J. Gutierrez, "Bayesian networks for probabilistic weather prediction," in *Proceedings of the 15th Eureopean Conference on Artificial Intelligence (ECAI 2002)*, 2002, pp. 695–699.

[20] K. Philippopoulos and D. Deligiorgi, "Statistical simulation of wind speed in Athens , Greece, based on Weibull and ARMA models," *Journal Of Energy*, vol. Vol. 3, pp. 151 – 158, 2009.

[21] J. Bect, Y. Phulpin, H. Baili, and G. Fleury, "On the Fokker-Planck equation for stochastic hybrid systems: Application to a wind turbine model," in *International Conference on Probabilistic Methods Applied to Power Systems, 2006 (PMAPS 2006)*, June 2006, pp. 1–6.

[22] E. Lee and S. Neuendorffer, "Tutorial: Building Ptolemy II models graphically," EECS Department, University of California, Berkeley, Tech. Rep. UCB/EECS-2007-129, Oct 2007.

[23] B. Silva and B. Krogh, "Formal verification of hybrid systems using CheckMate: a case study," in *Proceedings of the American Control Conference (ACC 2000)*, vol. 3, Aug 2000, pp. 1679–1683.

[24] A. Kurzhanskiy and P. Varaiya, "Ellipsoidal toolbox," EECS Department, University of California, Berkeley, Tech. Rep. UCB/EECS-2006-46, May 2006.

[25] M. Campi, S. Garatti, and M. Prandini, "The scenario approach for systems and control design," *Annual Reviews in Control*, pp. 149–157, 2009.

Martin Střelec received a MSc. degree in Information and Control Systems and a Ph.D. degree in Technical Cybernetics from University of West Bohemia, Pilsen, Czech Republic in 2004 and 2009, respectively. From 2004 to 2008, he was with Areva NP GmbH as a research engineer, where he developed new diagnostic methods for electromechanics actuators used in nuclear power plants. He has experience with modeling and diagnostics of power networks from several projects for Czech utility companies. Since 2010, he has been with Honeywell where he is involved in SmartGrids optimization, diagnostics, control and optimization of HVAC systems.

Karel Macek has worked for Honeywell since 2008. He contributed especially to HVAC diagnostics and optimization tasks where he won his Silver Bravo Award and Technical Achievement Award. Recently, he is focused also on Micro-Grid optimization and tools for demand response. Karel received his MSc. degree in Theoretical Computer Science from the Charles University in Prague in 2006 and BSc. in Applied Mathematics from Czech Technical University in 2004. Now, he is about to finish his Ph.D. studies in Applied Mathematics at Czech Technical University where he is focusing on the topic of data-based decision making. He is author and co-author of 8 conference contributions and 2 journal articles.

Alessandro Abate received a Laurea in Electrical Engineering in October 2002 from the University of Padova (Italy), an MS in May 2004 and a PhD in December 2007, both in Electrical Engineering and Computer Sciences, at UC Berkeley (USA). He has been an International Fellow in the CS Lab at SRI International in Menlo Park (USA), and a PostDoctoral Researcher at Stanford University (USA), in the Department of Aeronautics and Astronautics. Since June 2009, he has been an Assistant Professor at the Delft Center for Systems and Control, TU Delft - Delft University of Technology (The Netherlands).
His research interests are in the analysis, verification, and control of probabilistic and hybrid systems, and in their general application over a number of domains.

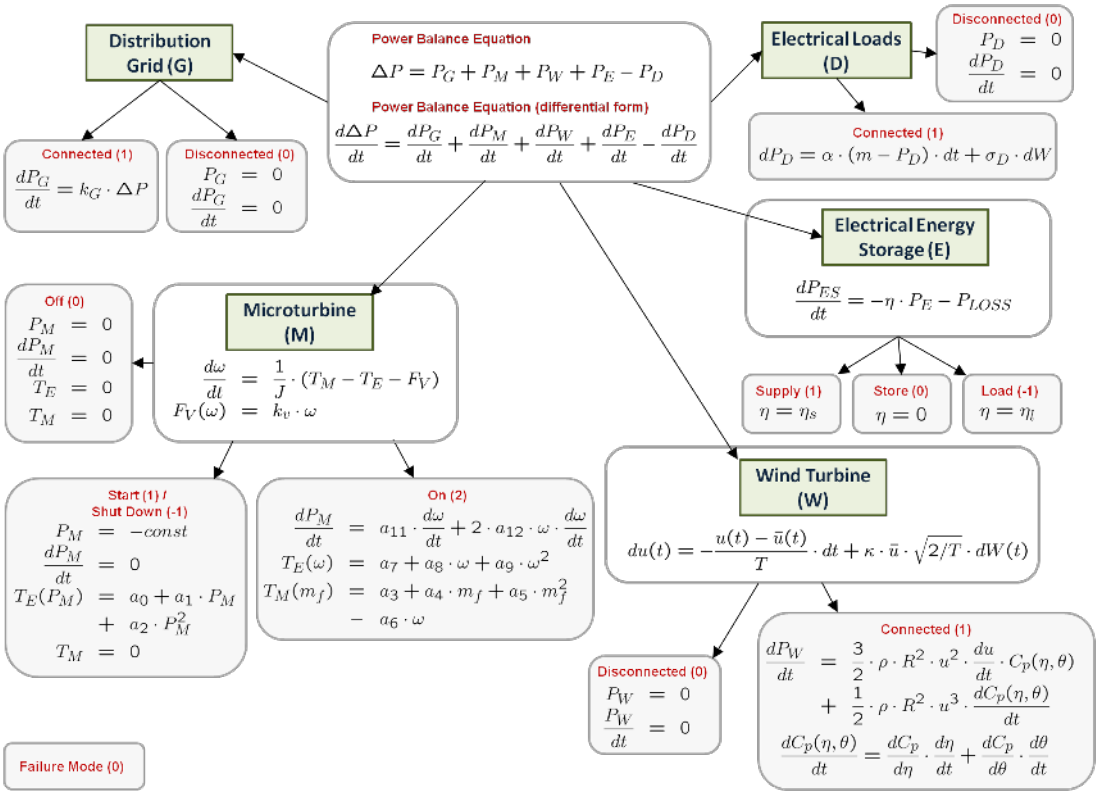

Fig. 7. The continuous dynamics (shaded blocks) associated to the devices (green rectangles) in the MG and their discrete modes of operations (red labels).

Appendix A
Continuous Dynamics of the Model

This section describes the continuous dynamics of the system captured by the graphical model shown in Figure 7. The root of the graph includes the power balance equation, where its terms refer to the devices incorporated in the MG. The continuous dynamics of the whole MG composes of the dynamics of the specific devices, represented in the vector [L G M W E D] – the value of this vector characterizes the global discrete modes of the SHS model, as discussed below. (also compare the vector value with Figure 2). Each green rectangular node represents a particular device in the MG. The leaves in the graph are explicitly associated to the continuous dynamics of a specific device, and thus contribute to the power balance equation at the root. For each leaf, the red label denotes the discrete operation mode and the number within brackets denotes the numerical code associated to that mode.

As an example, the global discrete mode [1 0 1 2 0 1] is obtained as follows. The distribution grid (G) is *Disconnected* from the MG, which is denoted as (G = 0). The label (G) relates to a green node and its value (0) determines the leaf of that node. The continuous dynamics for the grid is then

$$P_G = 0, \quad dP_G/dt = 0.$$

The microturbine is in its *On* mode (M = 1) and the corresponding continuous dynamics is captured in the device and in the leaf as follows:

$$\begin{aligned} \frac{d\omega}{dt} &= \frac{1}{J} \cdot (T_M - T_E - F_V), \\ F_V(\omega) &= k_v \cdot \omega, \\ \frac{dP_M}{dt} &= a_{11} \cdot \frac{d\omega}{dt} + 2 \cdot a_{12} \cdot \omega \cdot \frac{d\omega}{dt}, \\ T_E(\omega) &= a_7 + a_8 \cdot \omega + a_9 \cdot \omega^2, \\ T_M(m_f) &= a_3 + a_4 \cdot m_f + a_5 \cdot m_f^2 - a_6 \cdot \omega. \end{aligned}$$

The wind turbine is *Connected* to the MG (W = 1) and its corresponding continuous dynamics are

$$\begin{aligned} \frac{dP_W}{dt} &= \frac{3}{2} \cdot \rho \cdot R^2 \cdot u^2 \cdot \frac{du}{dt} \cdot C_p(\eta, \theta), \\ &+ \frac{1}{2} \cdot \rho \cdot R^2 \cdot u^3 \cdot \frac{dC_p(\eta, \theta)}{dt}, \\ \frac{dC_p(\eta, \theta)}{dt} &= \frac{dC_p}{d\eta} \cdot \frac{d\eta}{dt} + \frac{dC_p}{d\theta} \cdot \frac{d\theta}{dt}, \\ du(t) &= -\frac{u(t) - \bar{u}(t)}{T} dt + \kappa \bar{u} \sqrt{2/T} dW(t). \end{aligned}$$

The electrical energy storage device is disconnected from the MG and is storing the energy (E = 0, *Store* mode). The continuous dynamics for this mode are

$$\frac{dP_{ES}}{dt} = -P_{LOSS}.$$

Finally, an electrical load is *Connected* to the local power network (D = 1) and its dynamic is driven by the following stochastic differential equation:

$$dP_D = \alpha \cdot (m - P_D) \cdot dt + \sigma_D \cdot dW.$$